

Rigid Interpenetrating Polymer Network Foams Prepared from a Rosin-Based Polyurethane and an Epoxy Resin

Y. ZHANG,^{1,*} D. J. HOURSTON²

¹ Research Institute of Chemical Processing and Utilization of Forest Products, Nanjing 210037, People's Republic of China

² Institute of Polymer Technology and Materials Engineering, Loughborough, University of Technology, Loughborough, Leics., LE11 3TU, UK

Received 30 August 1996; accepted 6 April 1997

ABSTRACT: A series of rigid interpenetrating polymer network (IPN) foams, based on a rosin-based polyurethane and an epoxy resin, were prepared by a simultaneous polymerization technique. The changes in the chemical structure, dynamic mechanical properties, and morphology of the rigid IPN foams were investigated by Fourier transform infrared (FTIR) spectroscopy, dynamic mechanical thermal analysis, and scanning electron microscopy. The FTIR analysis showed clearly that the cure rate of the rosin-based rigid polyurethane foam and the epoxy resin were different and, as a result, these two networks formed sequentially in the final rigid IPN foams. All of the rigid IPN foams exhibited a single, broad glass transition that shifted to lower temperature as the epoxy resin content increased. The experimental composition dependence of T_g 's of the rigid IPN foams showed slight positive deviation from the Fox equation for homogeneous polymer systems. No phase separation was observed from the scanning electron microscopy investigation. It could be concluded that these two component networks were compatible in the final rigid IPN foams. This compatibility could be attributed to a graft structure in the polyurethane and the epoxy resin networks arising from the reaction of the hydroxyl groups of the epoxy resin with the isocyanate groups of MDI, and from the reaction of the hydroxyl groups of the polyols with the epoxide groups of the epoxy resin, as suggested by FTIR analysis. © 1998 John Wiley & Sons, Inc. *J Appl Polym Sci* 69: 271–281, 1998

Key words: polyurethane; epoxy resin; interpenetrating polymer networks; rigid foam; gum rosin; morphology; compatibility

INTRODUCTION

Since the first synthesis by Miller¹ in 1960, the term interpenetrating polymer networks (IPNs) has been used to describe the combination of crosslinked polymer networks in which at least

one polymer is synthesized and/or crosslinked in the immediate presence of the other.²

There are two principal routes for preparing IPNs, namely sequential and simultaneous polymerization of the two components.^{3,4} Sequential IPNs are generally prepared by swelling the first-formed network with the second monomer, which is then polymerized *in situ*. Simultaneous IPNs result from, of necessity, one-shot, one-stage processes.

IPNs, like most polymer/polymer systems, generally show phase separation⁵ as a consequence

Correspondence to: D. J. Hourston.

* Currently a visiting postdoctoral research fellow in the Loughborough University of Technology, Loughborough, UK.

Journal of Applied Polymer Science, Vol. 69, 271–281 (1998)

© 1998 John Wiley & Sons, Inc.

CCC 0021-8995/98/020271-11

of the low entropy change on mixing, which results in a positive value for the Gibbs free energy of mixing. The IPN technique can be a very effective method to improve the properties of existing polymer materials and to synthesize new ones with special properties. The compatibility of the two component polymers in an IPN is an important criterion in determining its physical properties.

Epoxy resins (ERs) are widely used as the matrices of high-performance composite materials because of their stiffness, chemical resistance, and high temperature stability. However, they are inherently brittle.⁶ Polyurethanes (PUs) are a versatile group of polymers prepared by the reaction of diisocyanates with hydroxyl-containing compounds. They can be used in a wide spectrum of polymeric products, including foams, elastomers, coating resins, adhesives, and fibers. However, their relative low thermal resistance and strength limit their applications. Therefore, several researchers have proposed^{7–20} IPN combinations to improve properties of PUs and ERs. Although a lot of work^{7–20} has been done on the synthesis and properties of PU/ER IPNs, most of it has focused on improving the brittleness of ERs. As far as rigid PU foams is concerned, to our knowledge, only one previous paper¹⁶ has dealt with this topic. Moreover, that work focused mainly on the mechanical properties of the PU/ER IPNs, and little work has been done on the structure and morphology of rigid PU/ER IPN foams.

Because world forecasts on both petroleum consumption and reserves point to exhaustion of supplies by the late 21st century, the use of natural renewable resources to substitute for chemicals now derived from petroleum has recently gained considerable importance.

The authors have synthesized²¹ a new kind of polyester polyol designed for making rigid PU foams from gum rosin—an abundant, renewable tree derivative. It was found^{21–23} that this kind of rosin-based rigid PU foam had some good mechanical and thermal properties. In this article, a series of rigid PU/ER IPN foams were synthesized from the rosin-based polyester polyol and using HCFC 141b, an alternative to CFC-11, as the blowing agent. Fourier transform infrared (FTIR) spectroscopy, dynamic mechanical thermal analysis (DMTA), and scanning electron microscopy (SEM) studies have been conducted to characterize the changes in chemical structure, dynamical mechanical properties, and morphology of the

rigid IPN foams during the cure process. The effect of epoxy content on the dynamical properties and morphology of the rigid IPN foams was also investigated. The present work aimed at providing an expanding understanding of the origin of the compatibility in these rigid PU/ER IPN foams.

EXPERIMENTAL

Materials

The materials used in this study are summarized in Table I. The rosin-based polyester polyol, the sucrose-based polyether polyol (R230), and ER were degassed at 60°C under vacuum for 12 h. HCFC 141b was used as the blowing agent to replace the CFC-11 that is believed to be an ozone-depleting agent. Triethanolamine and K54 were used as the cure catalysts of PU and ER, respectively.

Preparation of Rigid PU Foam and Rigid PU/ER IPN Foams

The rosin-based rigid PU foam itself was prepared²¹ *via* a one-shot method by mixing all of the ingredients listed in Table II together. The rigid PU/ER IPN foams were synthesized by adding varying amounts of ER (containing 5% of K54 curing catalyst) into the basic recipe of the neat rigid PU foam. The density of the rigid PU/ER IPN foam was controlled to be about 50 kg m⁻³ by varying the dosage of the blowing agent, HCFC 141b. The polyol, Epikote 828, silicone surfactant, blowing agent, and catalysts were mixed together first and then blended with MDI at a stirring speed of about 2000 rpm for 10 s. The mixture was then poured into a 20 × 8 (diameter) cm metal cylindrical mold preheated to 40°C. The polymer matrix foamed and cured within 1 to 2 min. After that, they were postcured in an air oven at 100°C for 1 h.

Testing Method

FTIR Spectral Measurements

FTIR spectroscopy was applied to characterize the changes in the chemical structure of the neat rigid rosin-based PU foam, the neat ER, and the PU/ER IPNs during the cure process. Thin films of

Table I Materials Used in This Study

Designation	Description	Source
RPP	Rosin-based polyether polyol; hydroxyl value: 400 mg KOH g ⁻¹	Synthesized by the authors ²¹⁻²³
	<p>$m, n, x, y \geq 1$</p>	
R230 (trade name: Daltolac)	Modified sucrose-based polyether polyol; hydroxyl value: 575 mg KOH g ⁻¹	ICI Polyurethanes
MDI (trade name: Suprasec DNR)	Diphenylmethane diisocyanate (MDI)-based composition, containing some higher functional isocyanates; NCO value: 30.8 wt %, functionality: 2.7	ICI Polyurethanes
HCFC 141b	1,1-Dichloro-1-fluoroethane	ICI Polyurethanes
Silicone surfactant	Polyether-modified polysiloxane (trade name: TEGOSTAB B8404)	Goldschmidt AG
TEA	Triethanolamine	Aldrich
K54	2,4,6-Tri(dimethyl aminomethyl) phenol	Air Products & Chemicals, Inc.
Epikote Resin 828	Bisphenol A-epichlorohydrin ($M_n < 700$)	Shell Co.

neat PU, neat ER, and PU/ER IPNs were prepared by casting the reaction mixtures directly onto potassium bromide disks before the cure reaction. All films were thin enough to yield good infrared spectra. They were cured at 100°C, and the FTIR spectra were measured by using a Mattson 3000 FTIR spectrometer at appropriate intervals during isothermal curing. One hundred and twenty-eight scans were collected at a 4 cm⁻¹ resolution in the mid-infrared range from 4000 cm⁻¹ to 600 cm⁻¹. Progress of the cure reactions was monitored by the characteristic absorption peaks of the isocyanate groups at 2278 cm⁻¹, the epoxide

groups at 914 cm⁻¹, and the hydroxyl and urethane groups at 3600 cm⁻¹ to 3100 cm⁻¹.

DMTA

DMTA was conducted using a Rheometric Scientific Dynamic Mechanical Thermal Analyzer (MK11) from 40°C to 200°C, with a heating rate of 4°C min⁻¹. These measurements were performed in the single cantilever bending mode at a fixed frequency (10 Hz). The dimensions of the specimens were approximately 8 × 9 × 5 mm.

Table II Basic Recipes for the Neat Rigid PU Foam and Rigid PU/ER IPN Foams

Designation	ER Content in the Rigid PU/ER IPN Foams				
	0 wt %	13.5 wt %	24.2 wt %	36.7 wt %	42.8 wt %
RPP	50	50	50	50	50
R230	50	50	50	50	50
Surfactant	2	2	2.6	3.2	3.6
MDI	154	154	154	154	154
TEA	4	4	4	4	4
HCFC 141b	30	33	37	48	53
Epikote 828	0	39	81	147	190
K54	5 wt % with respect to Epikote Resin 828				

RPP, rosin-based polyether polyol; TEA, triethanolamine.

SEM

Shredded specimens were mounted on aluminum stubs using conductive silver dag and were coated with gold to a thickness of about $0.015 \mu\text{m}$ in a sputter coater. Coated specimens were observed

in a scanning electron microscope (model 360; Cambridge Instruments, Nubloch, Germany) at a specimen angle of 0° .

RESULTS AND DISCUSSION

FTIR Spectral Analysis

Figure 1 shows the effect of cure time on the FTIR spectrum of neat rosin-based PU. In Figure 1, the isocyanate absorption at 2278 cm^{-1} is taken as the characteristic band.²⁴ Attention is also paid to the 3600 cm^{-1} to 3100 cm^{-1} region that contains overlapping absorption bands from hydroxyl groups and from the N—H bonds of urethane groups²⁵ and to the 1411 cm^{-1} absorption band that is associated with the isocyanurate rings,²⁴ formed by the trimerization of MDI.

As shown in Figure 1, the intensity of the isocyanate group absorption at 2278 cm^{-1} is high at the beginning of the cure reaction. As the cure reaction proceeds, it decreases rapidly and eventually disappears after 40 min, which indicates that the MDI isocyanate groups have nearly reacted completely with the hydroxyl groups of poly-

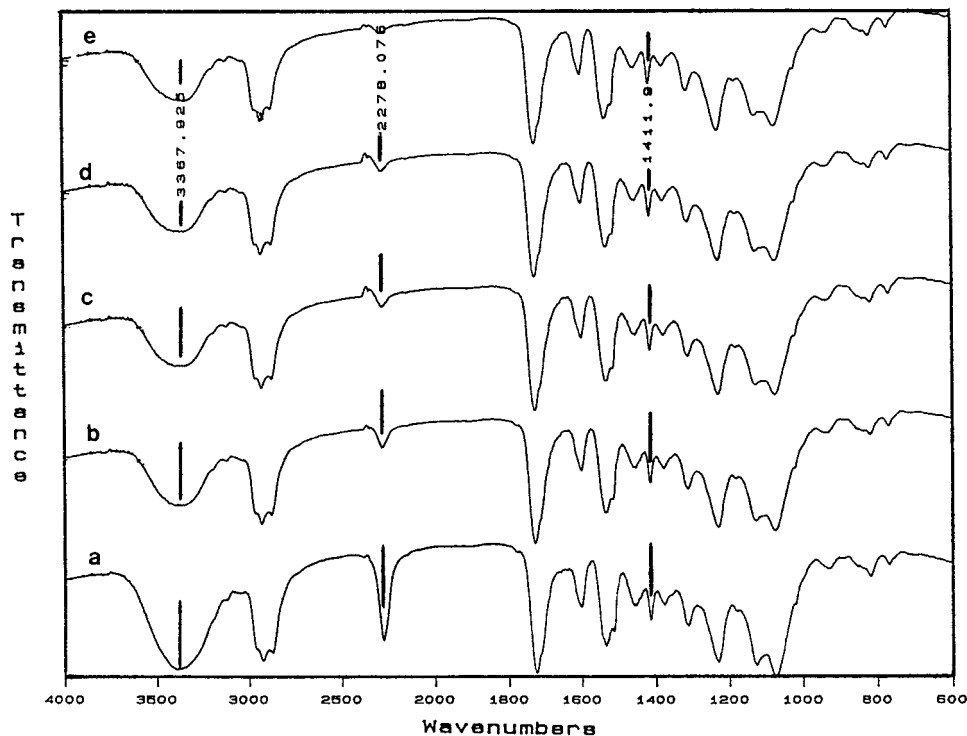


Figure 1 Change in FTIR spectra of pure rosin-based rigid PU foam with cure at 100°C . Cure time: (a) 2 min; (b) 10 min; (c) 20 min; (d) 40 min; (e) 120 min. Spectra are arbitrarily scaled and offset for display.

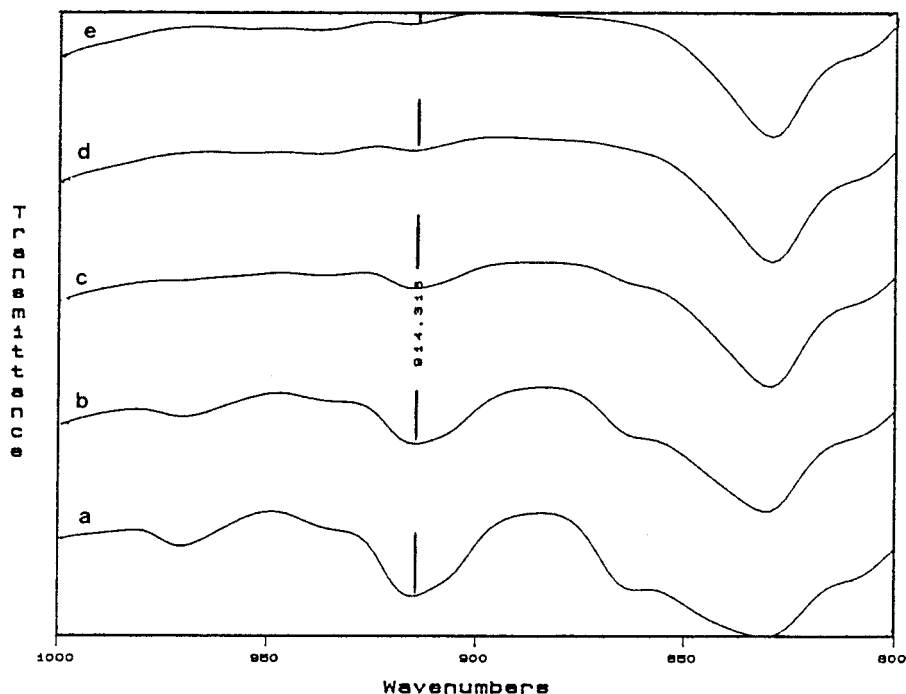


Figure 2 Change in FTIR spectra in 800 cm^{-1} to 1000 cm^{-1} region of pure ER with cure at 100°C . Cure time: (a) 0 min (uncured); (b) 40 min; (c) 60 min; (d) 120 min; (e) 180 min. Spectra are arbitrarily scaled and offset for display.

ester polyol and polyether polyol after this period of cure at 100°C . In this article, a ratio of NCO/OH of 1.4 was used to synthesize the pure rosin-based PU and the PU/ER IPNs. In addition, a tertiary amine was used as a catalyst. Therefore, it is expected^{24,26} that the excess MDI would be trimerized to form isocyanurate rings, which is confirmed from the absorption band at 1411 cm^{-1} in Figure 1.

At the same time, the broad absorption band centered at 3367 cm^{-1} decreases toward a constant value as the cure reaction proceeds. This broad band consists of hydroxyl group absorption and the N—H band of the urethane group absorption. The hydroxyl group absorption band is stronger than that of the N—H band of urethane group. Therefore, as more hydroxyl groups are consumed by reaction with isocyanate groups, forming urethane groups, this absorption band becomes weaker. It reaches a constant value after all the hydroxyl groups have reacted. It should be pointed out that the broad band centered at 3367 cm^{-1} also implies that strong hydrogen bonding exists among the urethane groups.

The region in the infrared spectrum associated with epoxide group absorption, between 800 cm^{-1} and 1000 cm^{-1} , is shown in Figure 2 for the neat

ER cured for different times. It was observed that the characteristic absorption band^{27,28} of the epoxide group at 914 cm^{-1} decreased gradually as the cure reaction proceeded. At a cure time of 120 min, the absorption band at 914 cm^{-1} reached a constant and small value.

In Figure 2, another interesting observation was that, as for pure ER, judged fully cured by DMTA measurements at a cure time of 120 min at 100°C , there remains, in fact, the absorption band of unreacted epoxide groups. This phenomenon²⁸ may be attributed to the topological constraints in highly crosslinked networks that render inaccessible a fraction of the epoxide groups during the cure process.

A comparison of the cure reaction of the neat PU and the neat ER showed that the cure reaction of PU was faster than that of the ER, which suggests that, in PU/ER IPNs, these two networks are formed more sequentially than simultaneously.

Figure 3 shows the change in the FTIR spectrum with a cure in the PU/ER IPN system containing 36.7 wt % of ER. As the cure reaction proceeds, the isocyanate band at 2280 cm^{-1} and the epoxide band at 914 cm^{-1} gradually decrease and then disappear. It should be noted that the isocya-

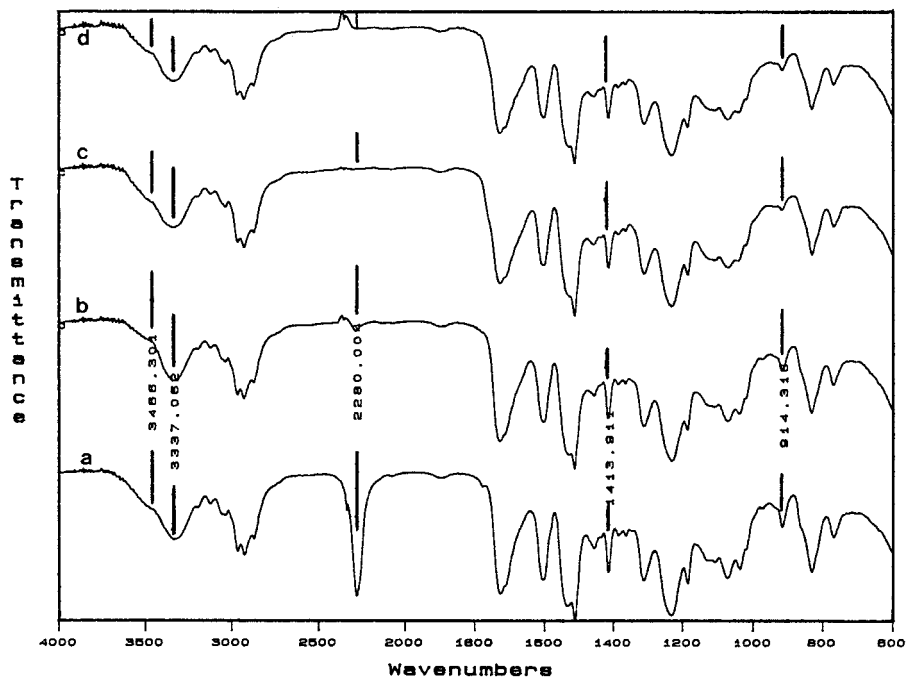


Figure 3 Change in FTIR spectra of the rosin-based PU/ER IPN rigid foam with cure at 100°C. Cure time: (a) 0 min (uncured); (b) 20 min; (c) 40 min; (d) 120 min. Spectra are arbitrarily scaled and offset for display.

nate groups have nearly all been consumed at a cure time of 20 min, whereas a considerable amount of epoxide groups remain unreacted, due to the different curing rates of these two components, as discussed previously. As a consequence, in the IPNs, these two networks gelled more sequentially than simultaneously. It was observed that a shoulder band at 3466 cm^{-1} appeared beside the N—H absorption band at 3337 cm^{-1} in the PU/ER IPNs. This could be attributed to the unreacted pendent hydroxyl groups of the ER. It should be pointed out that no absorption band has been observed at 2130 cm^{-1} , which is associated with the oxazolidinone structure,²⁴ suggesting that the isocyanate groups do not react with epoxide groups in these PU/ER IPN systems.

A comparison of the FTIR spectrum of neat PU, neat ER, and IPNs is shown in Figure 4. All of these three samples were cured for 40 min at 100°C. It was observed that, after 40 min of cure, the isocyanate group absorption band had completely disappeared in the IPN system, whereas some of the isocyanate groups remained unreacted in the pure PU system. This indicates that some of the hydroxyl groups of the ER have reacted with the isocyanate to form grafts^{16,19} between the PU component and the ER component of the PU/ER IPNs. This may be the reason why

the rosin-based PU has very good compatibility with the ER in these PU/ER IPNs. Compared with the FTIR spectrum of neat PU, a new shoulder band at 3508 cm^{-1} appears in the PU/ER IPN, which could be attributed to the stretching vibrations of the pendent hydroxyl group of the ER. This implies that the hydroxyl groups of the ER are not consumed completely by reaction with isocyanate groups. A trimerization reaction of MDI has also taken place in the PU/ER IPNs to form isocyanurate rings, which can be observed from the absorption band at 1411 cm^{-1} in Figure 4.

At a cure time of 40 min, the epoxide band of the PU/ER IPNs at 914 cm^{-1} has nearly disappeared, whereas in the neat ER system this band is still strong (Fig. 2), suggesting that the cure rate of ER in the PU/ER IPN is faster than that in the pure ER system. This could be attributed to the existence of a larger numbers of polyol hydroxyl groups in the IPNs, which could catalyze²⁹ the opening of the epoxide rings. According to the generally accepted curing mechanism of ERs,²⁹ when it is catalyzed by tertiary amines, such as K54 in the present work, the catalyst approaches one of the carbon atoms of the epoxide ring and attaches itself. This reaction is strongly catalyzed by the presence of hydroxyl groups, which provide hydrogen bonding for the epoxide oxygen. The

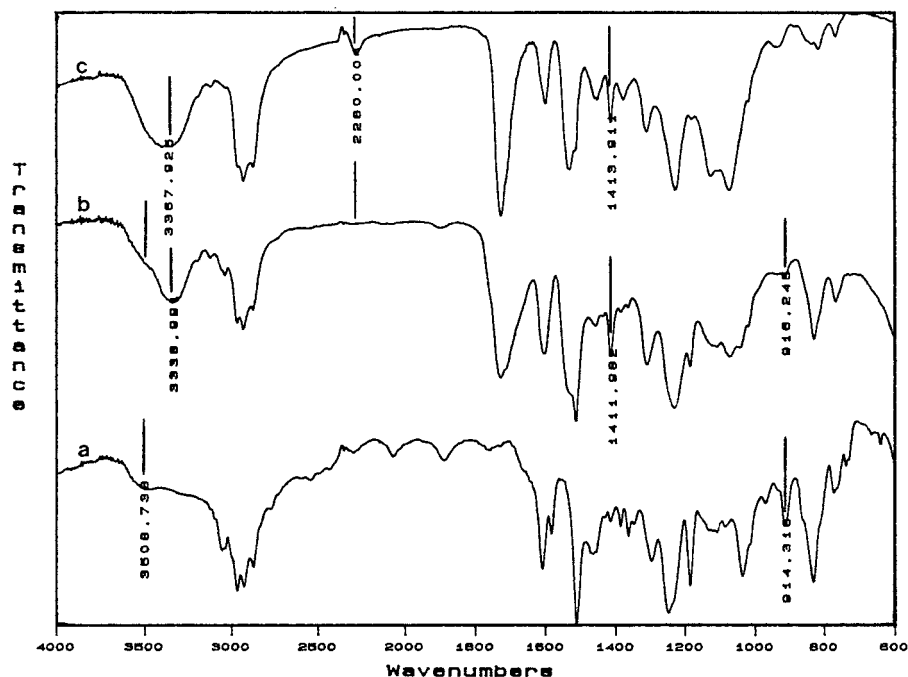


Figure 4 Comparison of FTIR spectra of pure ER, the pure rigid rosin-based PU foam, and the rigid PU/ER IPN foam with cure at 100°C for 40 min. (a) Pure ER; (b) PU/ER IPN; (c) Pure PU. Spectra are arbitrarily scaled and offset for display.

transition state is three-membered and favors the creation of an alkoxide ion from the original hydrogen donor. Then, the alkoxide ion reacts directly with another available epoxide group to

generate a new alkoxide ion. The process continues as a chain reaction. Lee and colleagues¹⁶ believed that, in the epoxy-PU system, if trace quantities of hydroxyl groups remain unreacted with

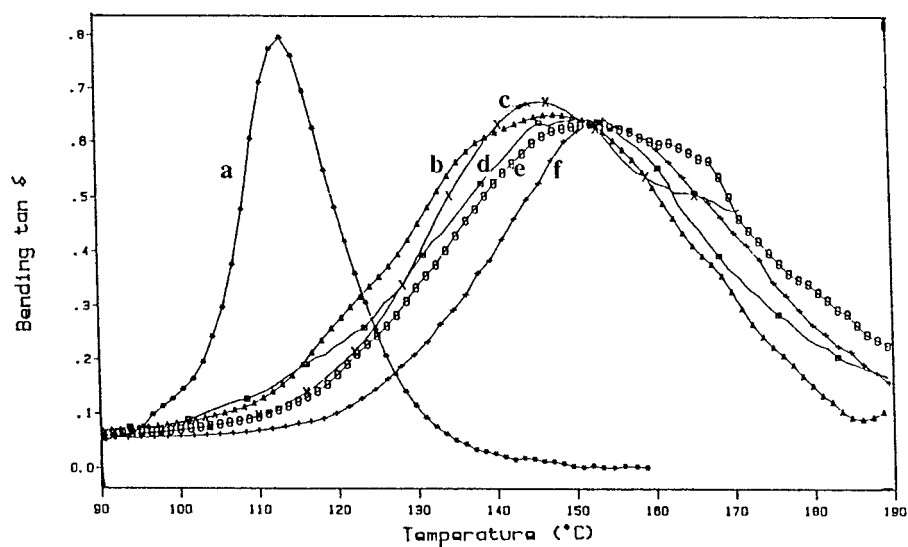


Figure 5 Tan δ against temperature of the rigid rosin-based PU/ER IPN foams with various ER contents: (a) 100%; (b) 42.8%; (c) 36.7%; (d) 24.2%; (e) 13.5%; (f) 0%.

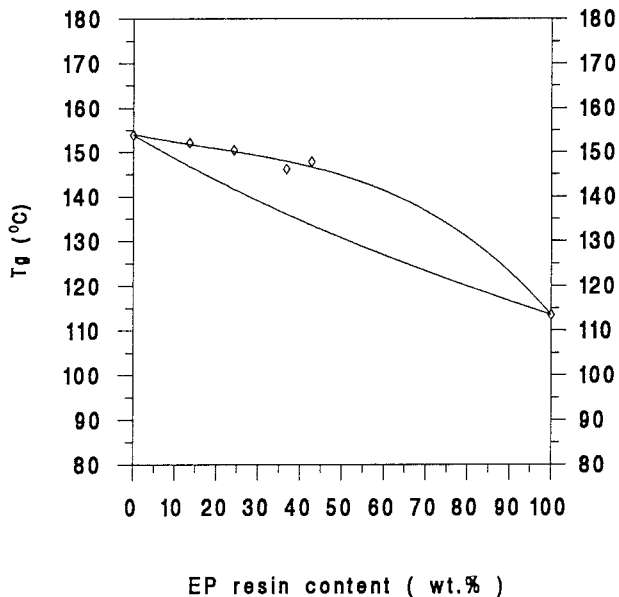


Figure 6 T_g values determined by DMTA and calculated from the Fox equation for the rigid PU/ER IPN foams. (\diamond) T_g determined by DMTA; (—) T_g calculated from Fox's equation.

isocyanate groups in the urethane formation stage, they are reacted in the epoxide ring-opening process in the ER cure stage. Then, grafts of the ER to the PU network results. The FTIR spectra in Figure 4 provided some direct evidence for the grafted structure in these PU/ER IPNs, which

together with the grafted structure formed from the reaction between the isocyanate groups of MDI and the hydroxyl groups of the ER is the most likely reason for the very high apparent compatibility of the ER and the PU shown by the presence of only a single glass transition in the DMTA spectra and the homogeneous morphology of the cell walls shown in the SEM micrographs. This will be discussed later.

Dynamic Mechanical Thermal Properties

DMTA studies were performed on the neat ER, the neat rosin-based rigid PU foams, and the rigid PU/ER IPN foams with different compositions and different cure times.

The loss tangent ($\tan \delta$) versus temperature plots of the neat PU foam, the neat ER, and the rigid PU/ER IPN foams with different compositions are shown in Figure 5. The neat PU and the neat ER exhibit T_g 's at 154°C and 113°C, respectively. It is noticeable that all of the rigid PU/ER IPN foams showed a single broad glass transition over a wide range of composition, with the $\tan \delta$ peaks of the IPNs shifting to lower temperature, toward the $\tan \delta$ peak of the neat ER, as the ER content increased. This is inconsistent with the work of Lee and coworkers¹⁶ on epoxy-modified PU rigid foam. This implies that the rigid PU/ER IPN foam system is miscible over a wide range of

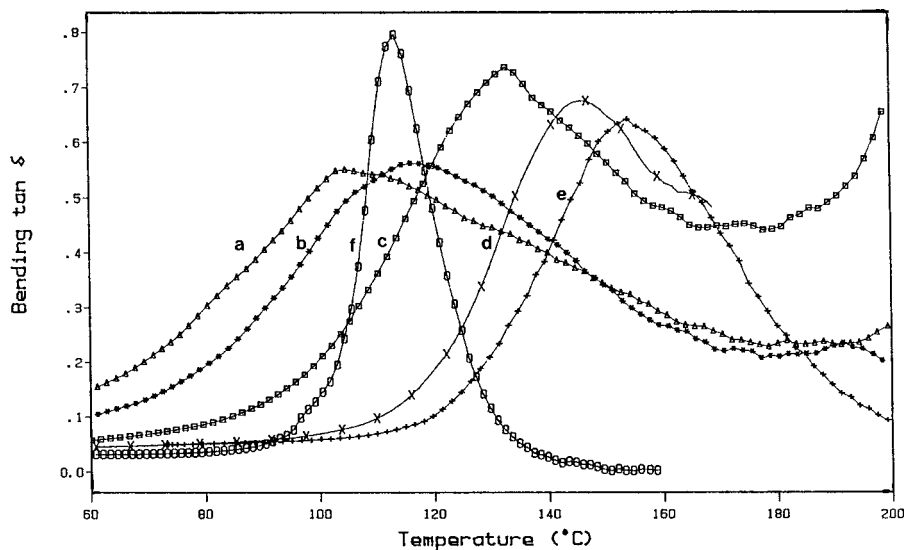


Figure 7 $\tan \delta$ versus temperature plots for the rigid rosin-based PU/ER IPN foams containing 36.7 wt % of ER cured at 100°C for different times. (a) 0 min (uncured); (b) 10 min; (c) 30 min; (d) 60 min. Curves for the neat rigid rosin-based PU foam (curve e) and for the neat ER (curve f) are also shown.

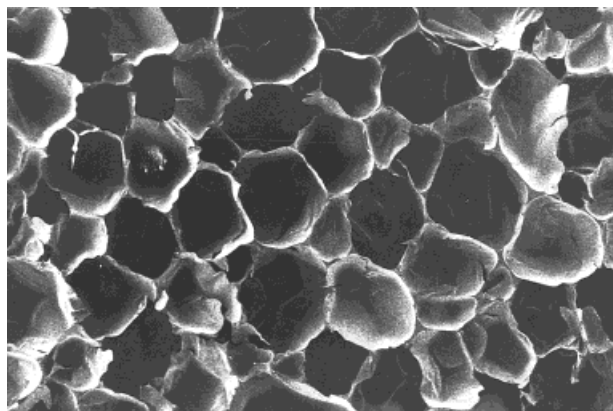


Figure 8 SEM micrograph of the rigid PU/ER IPN foam containing 13.5 wt % of ER.

composition. This apparent miscibility might be attributed to the possible graft structure of the PU and the ER networks through the reaction of the hydroxyl groups of the ER with the isocyanate groups of MDI, and through the reaction of the hydroxyl groups of the polyols with the epoxide groups of the ER, as discussed previously in relation to the FTIR spectra.

In multicomponent polymers systems, complete compatibility usually gives one single T_g that depends on the relative weight fractions of the two components and their respective T_g values. The compositional dependence of T_g of the PU/ER IPNs could be obtained according to the Fox³⁰ relationship:

$$1/T_g = W_1/T_{g1} + W_2/T_{g2}$$

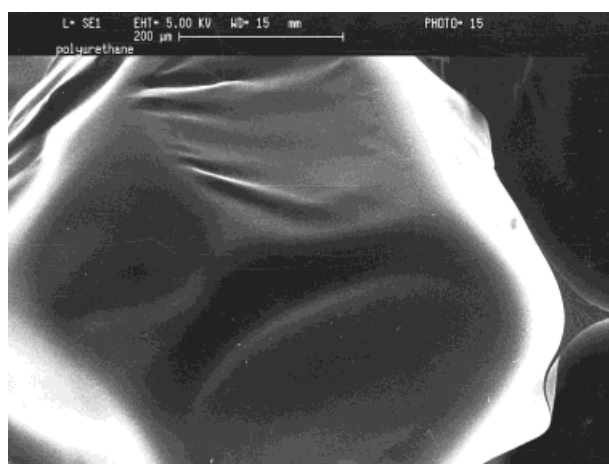
where W is the weight fraction of the components and T_g , T_{g1} , and T_{g2} are the glass transition temperatures of the IPNs, the neat PU, and the neat ER, respectively.

Figure 6 shows the variation of T_g with composition in the case of rigid PU/ER IPN foams and also the prediction³⁰ based on the Fox equation. Herein, the experimental values of T_g of the IPNs were taken from the temperatures corresponding to the $\tan \delta$ maxima in Figure 5. A slight positive deviation from the Fox equation was observed, which suggests that the interaction between the PU and the ER networks in these rigid PU/ER IPN foams is quite significant.

Figure 7 shows the $\tan \delta$ versus temperature plots for the rigid PU/ER IPN foam containing 36.7 wt % of ER cured at 100°C for different times.

For the sake of comparison, data for the neat rigid PU foam and for the neat ER are also presented.

It is apparent that the $\tan \delta$ peaks shift, as expected, to a higher temperature as the cure reaction proceeds. At the beginning of the cure reaction, the T_g of the rigid PU/ER IPN foams is even lower than that of neat ER. Because the cure rate of ER is slower than that of PU, as suggested by the FTIR spectra, it could be imagined that, at the beginning of the cure reaction, some of the ER remained unreacted and acted as a plasticizer, leading to lower T_g values of the IPNs. As the cure reaction proceeded, the PU network was cured fully first, and then the ER network was formed, resulting in an increase in the T_g of the IPNs.



(a)



(b)

Figure 9 SEM micrographs of the cell walls of (a) the neat rosin-based PU rigid foam and (b) the PU/ER IPN rigid foam containing 13.5 wt % of ER.

After a 1 h cure at 100°C, the T_g of the rigid IPN foams remained unchanged, which suggested a full cure had been reached, as was indicated by the FTIR spectra in Figure 3.

SEM

A SEM micrograph of a rigid PU/ER IPN foam is shown in Figure 8. A fairly uniform cell structure was observed for this rigid IPN foam, which had smooth cell wall surfaces like the rigid rosin-based PU foam (Fig. 9). By careful observations of the cell wall surfaces of these rigid PU/ER IPN foams with different ER contents and with different cure times at higher magnifications in SEM (as shown in Figs. 10 and 11), no resolvable phase



(a)



(b)

Figure 10 SEM micrographs of the cell wall surfaces of the rigid PU/ER IPN foams with different ER contents: (a) 0 wt % and (b) 36.7 wt %.



(a)



(b)

Figure 11 SEM micrographs of the cell wall surfaces of the rigid PU/ER IPN foam containing 36.7 wt % of ER cured for (a) 10 min and (b) 1 h.

structure was observed, which indicated that PU and ER components were completely miscible and formed a single phase in the final IPN foams. The observation is in good agreement with DMTA and FTIR analyses.

CONCLUSIONS

1. The cure rate of the rosin-based rigid PU foam was faster than that of the ER. As a result, these two networks are formed more sequentially than simultaneously in the rigid PU/ER IPN foams.
2. All of the rigid PU/ER IPN foams exhibited a single, broad glass transition that shifted

to lower temperature as the ER content increased. The experimental composition dependence of T_g of the rigid IPN foams showed a slight positive deviation from the Fox equation for homogeneous polymer systems. DMTA data indicated that the rosin-based PU and the ER are compatible in the rigid IPN foams.

3. SEM observations further confirmed that no phase separation existed in the rigid PU/ER IPN foams.
4. FTIR data suggested that a graft structure between the PU and the ER networks may be formed through the reaction of the hydroxyl groups of the ER with the isocyanate groups of MDI, and through the reaction of the hydroxyl groups of the polyols with the epoxide groups of the ER that could be the reason for the good compatibility of the PU and EP networks in these rigid IPN foams.

The authors acknowledge, with gratitude, the National Natural Science Foundation of China and The British Council for financial support. The authors also wish to thank ICI Polyurethanes for the kind provision of materials.

REFERENCES

1. J. R. Miller, *J. Chem. Soc.*, 1311 (1960).
2. L. H. Sperling, *Interpenetrating Polymer Networks and Related Materials*, Plenum Press, New York, 1981.
3. D. A. Thomas and L. H. Sperling, in *Polymer Blends*, Vol. 2, D. R. Paul and S. Newman, Eds., Academic Press, New York, 1978.
4. J. M. Widmaier and L. H. Sperling, *Br. Polym. J.*, **16**, 46 (1986).
5. L. H. Sperling, *J. Polym. Sci. Polym. Symp.*, **60**, 175 (1977).
6. C. A. May, Ed., *Epoxy Resin Chemistry and Technology*, Marcel Dekker, New York, 1988.
7. L. H. Sperling, *Polym. Eng. Sci.*, **25**, 517 (1985).
8. K. C. Frisch, D. Klempner, and S. K. Mukherjee, *J. Appl. Polym. Sci.*, **18**, 689 (1974).
9. E. F. Cassidy, H. X. Xiao, K. C. Frisch, and H. L. Frisch, *J. Polym. Sci. Polym. Chem. Ed.*, **22**, 2667 (1984).
10. E. F. Cassidy, H. X. Xiao, K. C. Frisch, and H. L. Frisch, *J. Polym. Sci. Polym. Chem. Ed.*, **22**, 1839 (1984).
11. K. H. Hsieh and J. L. Han, *J. Polym. Sci. B.*, **28**, 623 (1990).
12. K. H. Hsieh and J. L. Han, *J. Polym. Sci. B.*, **28**, 783 (1990).
13. R. Pernice, K. C. Frisch, and R. Navare, *J. Cell. Plast.*, **18**, 121 (1982).
14. D. Klempner, L. Berkowski, K. C. Frisch, K. H. Hsieh, and R. Ting, *Rubber World*, **192**, 16 (1985).
15. D. Klempner, B. Muni, M. Okoroafor, and K. C. Frisch, *Advances in Interpenetrating Polymer Networks*, Vol. II, Technomic Publishing, 1990, p. 1.
16. Y. Lee, W. Ku, J. Tsou, K. Wei, and P. Sung, *J. Polym. Sci.: Part A: Polym. Chem.*, **29**, 1083 (1991).
17. K. H. Hsieh, Y. C. Chiang, Y. C. Chern, W. Y. Chiu, and C. C. M. Ma, *Angew. Makromol. Chem.*, **193**, 89 (1991).
18. K. H. Hsieh, Y. C. Chiang, Y. C. Chern, W. Y. Chiu, and C. C. M. Ma, *Angew. Makromol. Chem.*, **194**, 15 (1992).
19. Y. C. Chern, K. H. Hsieh, C. C. M. Ma, and Y. G. Gong, *J. Mater. Sci.*, **29**, 5435 (1994).
20. N. A. Prakash, Y. M. Liu, B. Z. Jang, and J. B. Weng, *Polym. Comp.*, **15**, 479 (1994).
21. Y. Zhang, Y. Jin, Z. Liu, L. Bi, and D. Wang, *Chemistry and Chemical Engineering of Forest Products*, **11**, 203 (1991).
22. Y. Zhang, S. Shang, X. Zhang, D. Wang, and D. J. Hourston, *Polymer International*, **42**, 349 (1997).
23. Y. Zhang, S. Shang, X. Zhang, D. Wang, and D. J. Hourston, *J. Appl. Polym. Sci.*, **59**, 1167 (1996).
24. R. Merten, D. Lauerer, G. Braum, and M. Dahm, *Angew. Makromol. Chem.*, **101**, 337 (1967).
25. S. Lu, E. M. Pearce, and T. K. Kwei, *Polymer*, **36**, 2435 (1995).
26. G. Oertel, *Polymer Handbook*, 2nd ed., Hanser Publishers, 1993.
27. B. S. Kim and T. Inoue, *Polymer*, **36**, 1985 (1995).
28. F. Meyer, G. Samz, A. Eceiza, I. Mondragon, and J. Mijovic, *Polymer*, **36**, 1407 (1995).
29. H. Lee and K. Neville, *Handbook of Epoxy Resins*, McGraw-Hill, New York, 1972.
30. T. G. Fox, *Bull. Am. Phys. Soc.*, **1**, 123 (1956).